MASS AND MOMENTUM TURBULENT TRANSPORT EXPERIMENTS

B. V. Johnson and R. Roback
United Technologies Research Center

INTRODUCTION

An experimental study of mixing downstream of axial and swirling coaxial jets is being conducted to obtain data for the evaluation and improvement of turbulent transport models currently employed in a variety of computational procedures used throughout the propulsion community. The nonswirling coaxial jet study was completed under Phase I and is reported in Reference 1. The swirling coaxial jet study was conducted under Phase II of the contract and is reported in Reference 2. A TEACH code was acquired, checked out for several test cases, and is reported in Reference 3. A study to measure length scales and to obtain a limited number of measurements with a blunt trailing edge inlet is being conducted under Phase III of the contract and HOST sponsorship. Results from Phases I and II have also been presented in References 4, 5 and 6.

PHASE III OBJECTIVES

The Phase III effort was directed toward (1) the aquisition of length scale and dissipation rate data that will provide more accurate inlet boundary conditions for the computational procedures and a data base to evaluate the turbulent transport models in the near jet region where recirculation does not occur and (2) the acquisition of mass and momentum turbulent transport data with a blunt inner-jet inlet configuration rather than the tapered inner-jet inlet employed in Phases I and II.

Mass and momentum turbulent transport data was obtained downstream of the blunt inner-jet inlet configuration, using the laser velocimeter/laser induced fluoresence measurement techniques employed in the previous experiments with swirling and nonswirling flow conditions. The velocities, concentrations, mass turbulent transport and momentum turbulent transport results obtained downstream of the blunt inner-jet inlet configuration for the nonswirling flow condition were not significantly different from those obtained with the tapered inner-jet inlet. The results will be presented and compared with the Reference 1 results in the forthcoming Phase III interim summary report.

The measurement technique generally used to obtain approximate integral length and micro scales of turbulence and dissipation rates was recently computerized at UTRC. This computerized data aquisition and reduction procedure was then used to obtain length scale and dissipation rate data for three test configurations. The data and results obtained with the tapered inner jet inlet configuration and the nonswirling flow condition will be discussed in the following sections.

---

*Performed under Contract NAS3-22771.

Data Analysis Formulation

With Taylor's hypothesis, the temporal variation of a one dimensional velocity fluctuation is related to a spatial variation by the convective velocity, U. This is also referred to as the frozen-turbulence approximation (Ref. 7). The autocorrelation is defined

$$R(\tau) = u(t) \quad u(t+\tau)/u'^2$$

An integral scale and an approximate micro scale of turbulence and an eddy dissipation rate are related to the autocorrelation. The integral scale of turbulence is:

$$L1 = U \quad \int_0^\infty R(\tau)\, d\tau$$

A second integral scale of turbulence is also obtained directly from spectrum (Ref. 7)

$$L2 = (U/4) \lim_{n \to 0} [E(n)/u'^2]$$

The microscale length of turbulence, λ, is defined as the intercept of the parabola that matches $R(\tau)$ at $\tau = 0$, i.e.,

$$R(\tau) = 1 - (\tau U/\lambda)^2$$

The dissipation rate, ϵ, is related to the microscale of turbulence, the rms velocity and the fluid kinematic viscosity, ν:

$$\epsilon = 30 \quad \nu u'^2/\lambda^2$$

Although the autocorrelation/microscale relations shown above will lead to a dissipation rate, the determination of the curvature of $R(\tau)$ at $\tau = 0$ is often difficult and sometimes ambiguous. Another relationship for the dissipation rate is obtained directly from the one-dimensional velocity turbulent energy spectra

$$1/\lambda^2 = (2\pi)/(U^2 u'^2) \int_0^\infty n^2 \, E(n) \, dn$$

where $E(n)$ is the turbulent kinetic energy per frequency cycle of one velocity component at frequency n. Thus the approximate dissipation rate is more easily obtained with an independent spectrum measurement.

An autocorrelation for the spectral data is also constructed from the Fourier transform of the energy spectral distribution using a computer routine which is part of the data reduction program. The Fourier transform which produces the spatial correlation is

$$R(\tau) = \int_0^\infty e^{i\tau\omega} \, E(\omega) \, d\omega$$

The information flow chart for the computerized length scale measurement technique is shown in Figure 1.

Test Conditions and Apparatus

The length scale and dissipation rate measurements were conducted in the UTRC coaxial flow facility (Figure 2) using water as the working fluid. The flow conditions and geometries were identical to those employed in Reference 1, i.e. U (inner) = 0.52 m/s and U (annular) = 1.66 m/sec and with a Reynolds number of 35,000 based on the duct diameter and the average velocity.

A sketch of the inlet and measurement locations is shown in Figure 3. The swirler was not installed for the measurements discussed herein. Mean, fluctuating and spectral measurements of the axial velocity were obtained in the regions without recirculation at z = -41, 5, 51 and 102 mm from the inlet plane. Mass and momentum turbulent transport data was obtained at the latter three locations during Phase I (Reference 1). Standard hot film constant resistance measurement procedures were used to aquire the data. The water was filtered to prevent particles in the water from attaching to the probe and altering the probe calibration curve.

Results

The mean and fluctuating axial velocity measurements obtaining at the four axial locations are presented in Figures 4 and 5 and compared with results from Reference 1 obtained with a laser velocimeter. The agreement between the two sets of measurements is excellent. The conclusion from this comparison is that the hot film data aquisition and reduction procedure for obtaining mean and fluctuating velocities reproduces the previous results with acceptable accuracy.

The dissipation rate distributions for the four axial locations are presented in Figure 6. Note the dissipation rates at the center of the inner jet and the annular jets are approximately the same at z = -41 and 5 mm from the inlet plane. At z = 5.1 mm, the dissipation rate across the inlet varies by 2 1/2 orders of magnitude. This radial variation decreases to less than one order of magnitude (by increasing the lower dissipation rates and decreasing the higher dissipation rates) at z = 102 mm from the inlet plane. As expected the locally high and low dissipation rates are associated with high and zero axial velocity shear rates, respectively.

The integral length and micro scales of turbulence are presented in Figure 7. The integral scales L1 and L2, defined on the figure, were both determined as part of the computerized data reduction procedure. Note that the integral scales determined by both methods are in generally good agreement. The largest difference between the two scales is about 20 percent and occured at z = 102 mm. This is a location with long wave length eddies occuring over a moderate frequency range. The differences between the two integral length scales are generally less than ten percent with the integral scale determined from the integration of the auto correlation always being greater. The integral scales of turbulence in the inner jet inlet were 9 to 12 mm, approximately half the tube diameter and compatible with length scales reported in Reference 7 for previous work by Laufer.

The micro scales of turbulence ,λ, were 15 to 40 percent of the integral length scales. The ratio of micro scale to integral scale inside the inlet duct (z = -41 mm) was somewhat greater than measured by Laufer for a two-dimensional duct, i.e. : 15 percent of the UTRC circular duct diameter compared to 10 percent of the Laufer 2-d slot height. Thus, the present results in the duct appear to be reasonably

compatable with previous studies. The micro scale of turbulence does not vary much ($1 < \lambda < 3.8$mm) compared to the integral scale of turbulence. For the two measurement locations downstream of the inlet, the ratio of the maximum to minimum microscales ($2 < \lambda < 4$mm) is only half the ratio of the integral length scales ($4.2 < L < 19$).

REFERENCES

1. Johnson, B. V. and J. C. Bennett: Mass and Momentum Turbulent Transport Experiments with Confined Coaxial Jets. NASA Contractor Report CR-165574 (Interim Summary Report), November 1981.

2. Roback, R. and B. V. Johnson: Mass and Momentum Turbulent Transport Experiments with Confined Swirling Coaxial Jets. NASA Contractor Report CR-168252 (Interim Summary Report), August 1983.

3. Chiapetta, L. M.: User's Manual for a TEACH Computer Program for the Analysis of Turbulent, Swirling Reacting Flow in a Research Combustor. UTRC Report R83-915540-27 prepared under NASA Contract NAS3-22771, September 1983.

4. Johnson, B. V. and J. C. Bennett: Mass and Momentum Turbulent Transport Experiments with confined Coaxial Jets. Presented at Fourth Symposium on Turbulent Shear Flows, Karlsruhl, September 12-14, 1983.

5. Johnson, B. V. and J. C. Bennett: Statistical Characteristics of Velocity, Concentration, Mass Transport and Momentum Transport for Coaxial Jet Mixing in a Confined Duct. ASME Journal of Engineering for Gas Turbines and Power. Vol. 106, p. 121-127, January 1984.

6. Johnson, B. V. and R. Roback: Mass and Momentum Turbulent Transport Experiments with Confined Swirling Coaxial Jets: Part I. AIAA Preprint 84-1380. Presented at 20th Joint Propulsion Conf. Cincinnati, Ohio. June 11 - 13, 1984.

7. Hinze, J. O.: Turbulence, McGraw-Hill, 1959

FIG. 1

INFORMATION FLOW CHART FOR COMPUTERIZED LENGTH SCALE MEASUREMENT TECHNIQUE

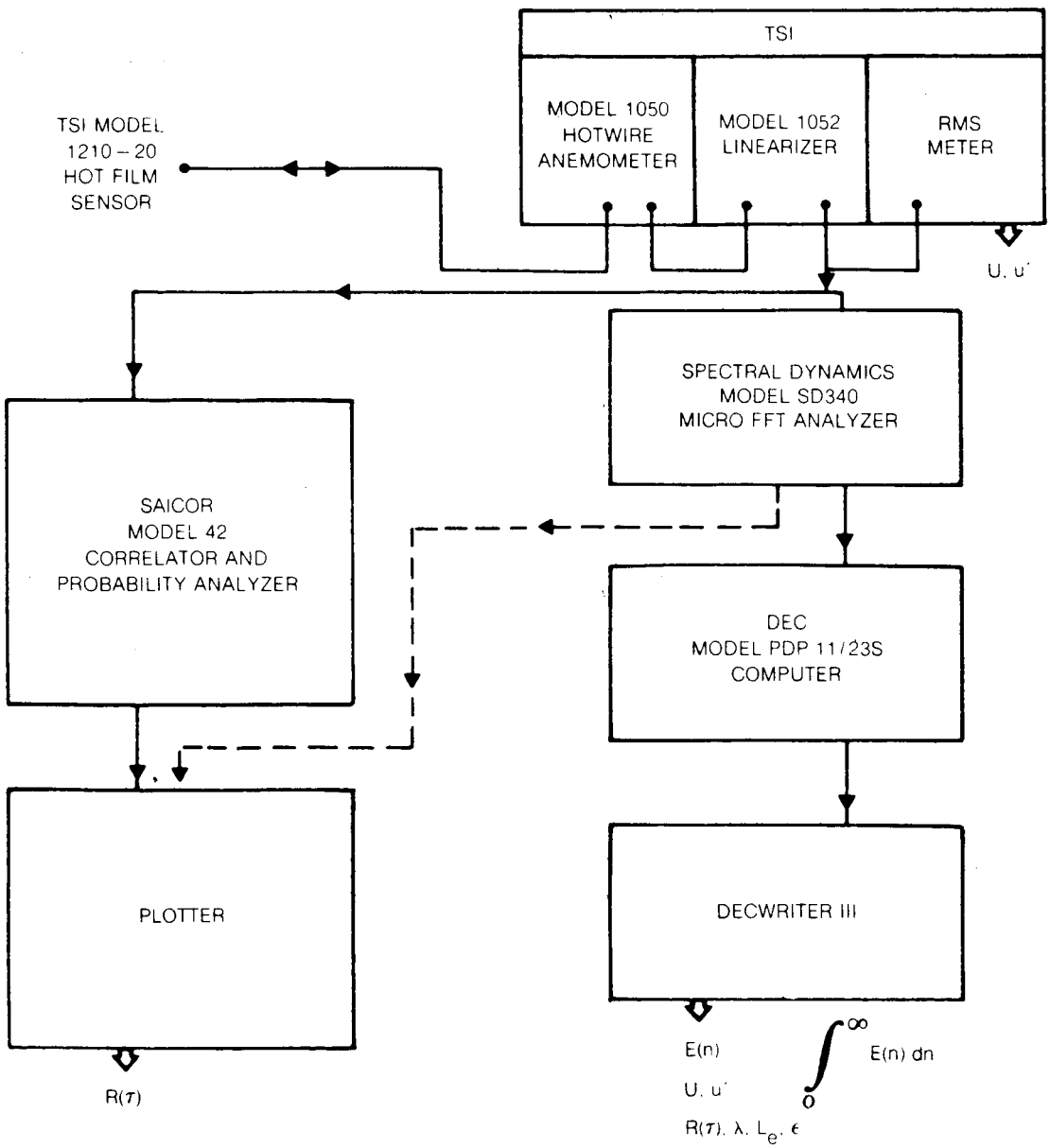

FIG. 2

SKETCH OF COAXIAL FLOW FACILITY

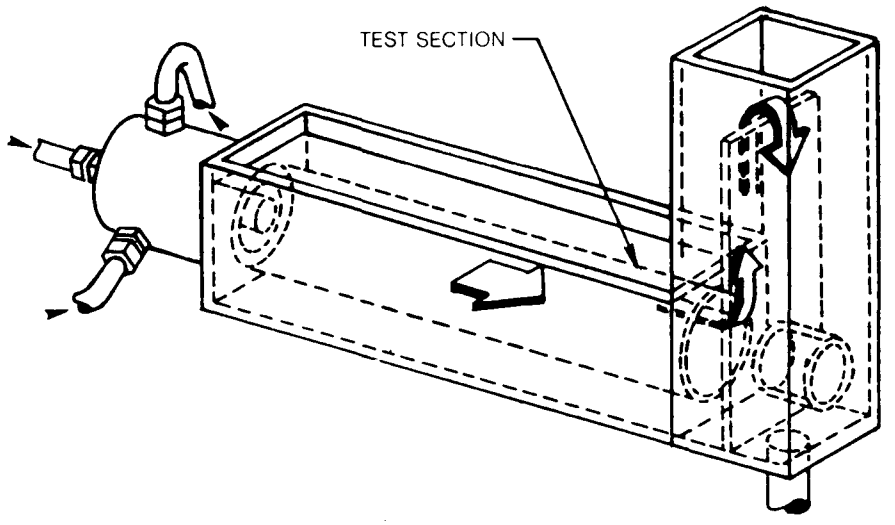

FIG. 3

SKETCH OF LENGTH SCALE MEASUREMENT ARRANGEMENT

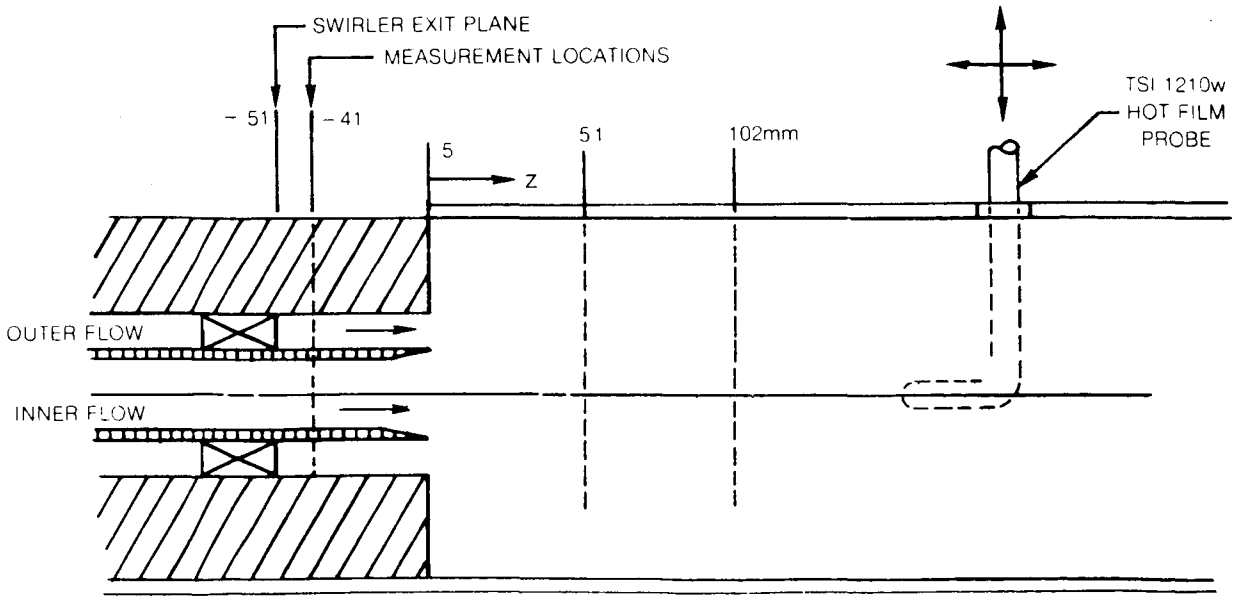

FIG. 4

MEAN AXIAL VELOCITY PROFILES FOR NONSWIRLING FLOW WITH TAPERED INNER JET INLET

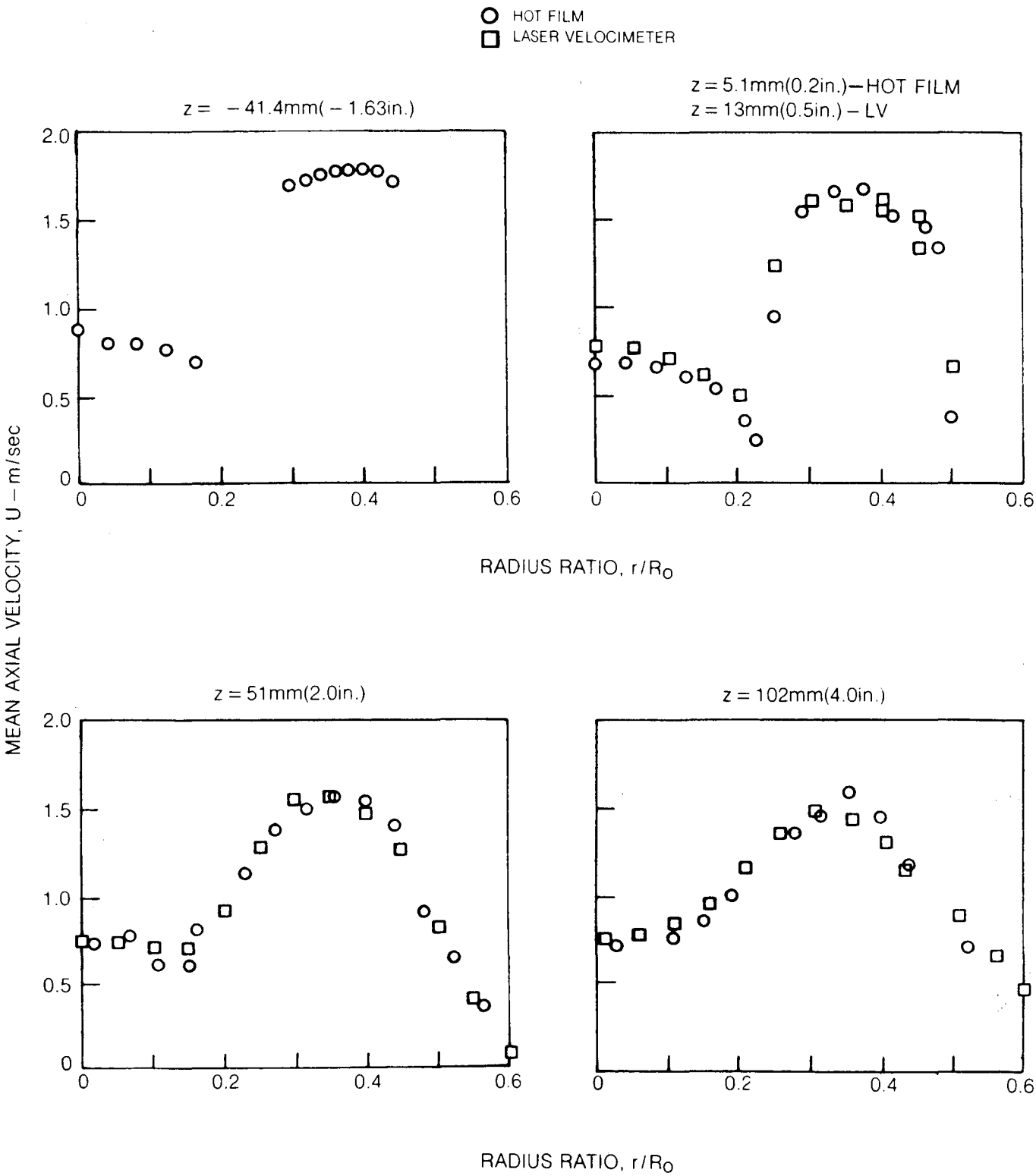

FIG. 5

FLUCTUATING AXIAL VELOCITY PROFILES FOR NONSWIRLING FLOW WITH TAPERED INNER JET INLET

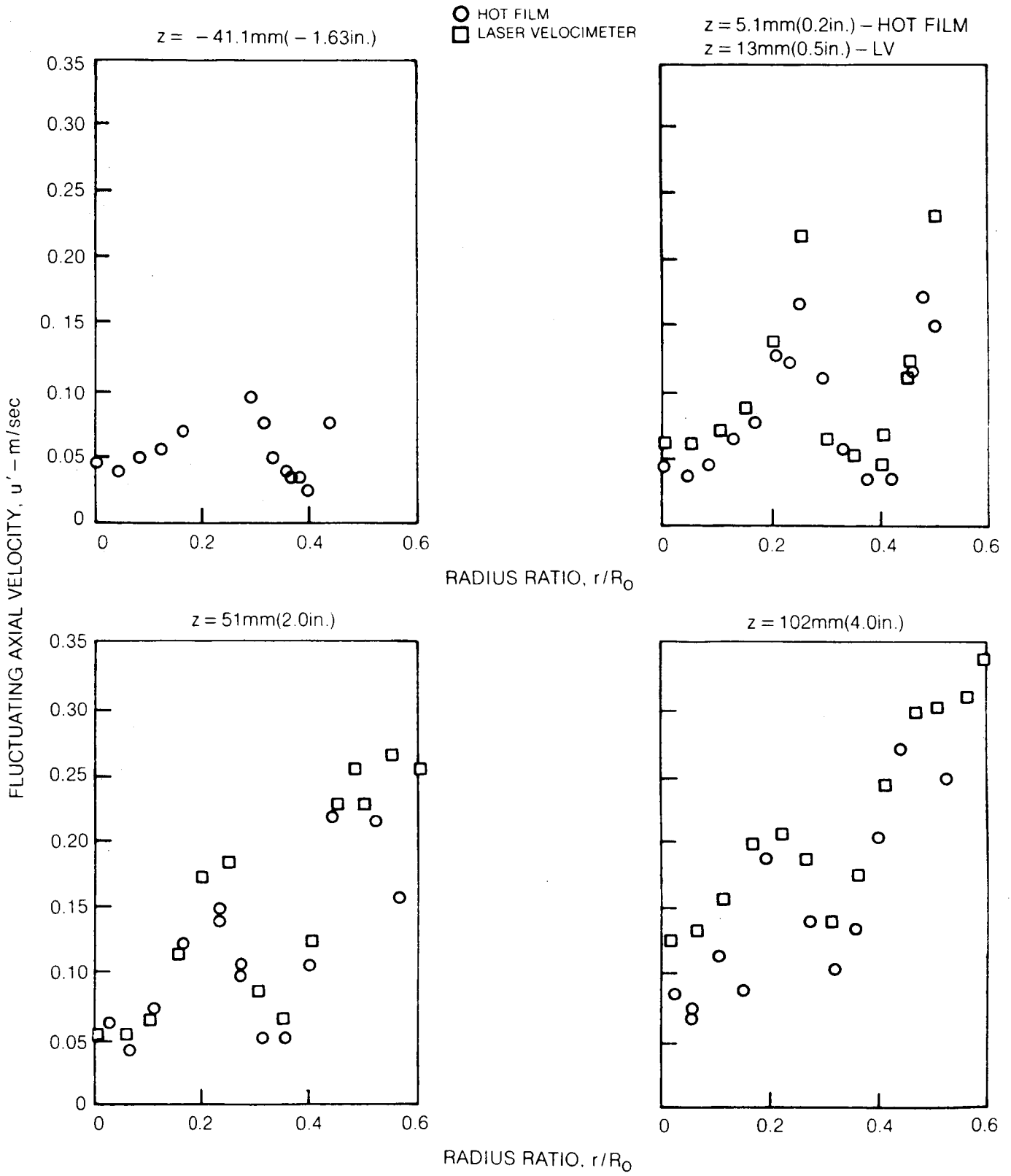

FIG. 6

DISSIPATION RATE FOR NONSWIRLING FLOW WITH TAPERED INNER JET INLET

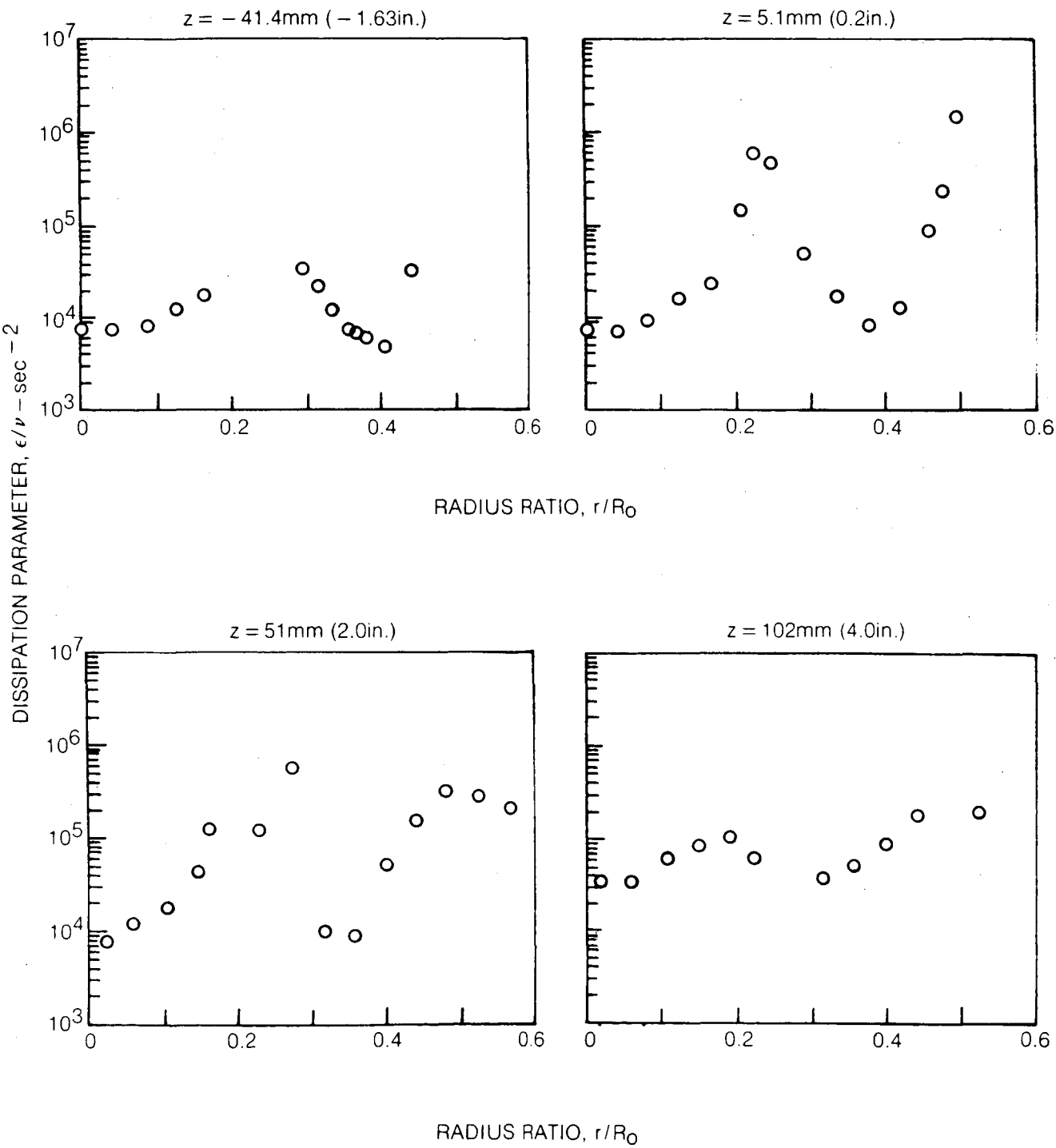

FIG. 7

LENGTH SCALE DISTRIBUTION FOR NONSWIRLING FLOW WITH TAPERED INNER JET INLET